Title

Phosphoinositide 3-Kinase Binds to TRPV1 and Mediates NGF-stimulated TRPV1 Trafficking to the Plasma Membrane

Journal

The Journal of General Physiology, 128(5)

ISSN

0022-1295

Authors

Stein, Alexander T
Ufret-Vincenty, Carmen A
Hua, Li
et al.

Publication Date

2006-11-01

DOI

10.1085/jgp.200609576

Peer reviewed

Phosphoinositide 3-Kinase Binds to TRPV1 and Mediates NGF-stimulated TRPV1 Trafficking to the Plasma Membrane

Alexander T. Stein,[1] Carmen A. Ufret-Vincenty,[2] Li Hua,[2] Luis F. Santana,[2] and Sharona E. Gordon[2]

[1]Graduate Program in Neurobiology and Behavior and [2]Department of Physiology and Biophysics, University of Washington, Seattle, WA 98195

Sensitization of the pain-transducing ion channel TRPV1 underlies thermal hyperalgesia by proalgesic agents such as nerve growth factor (NGF). The currently accepted model is that the NGF-mediated increase in TRPV1 function during hyperalgesia utilizes activation of phospholipase C (PLC) to cleave PIP2, proposed to tonically inhibit TRPV1. In this study, we tested the PLC model and found two lines of evidence that directly challenge its validity: (1) polylysine, a cationic phosphoinositide sequestering agent, inhibited TRPV1 instead of potentiating it, and (2) direct application of PIP2 to inside-out excised patches dramatically potentiated TRPV1. Furthermore, we show four types of experiments indicating that PI3K is physically and functionally coupled to TRPV1: (1) the p85β subunit of PI3K interacted with the N-terminal region of TRPV1 in yeast 2-hybrid experiments, (2) PI3K-p85β coimmunoprecipitated with TRPV1 from both HEK293 cells and dorsal root ganglia (DRG) neurons, (3) TRPV1 interacted with recombinant PI3K-p85 in vitro, and (4) wortmannin, a specific inhibitor of PI3K, completely abolished NGF-mediated sensitization in acutely dissociated DRG neurons. Finally, simultaneous electrophysiological and total internal reflection fluorescence (TIRF) microscopy recordings demonstrate that NGF increased the number of channels in the plasma membrane. We propose a new model for NGF-mediated hyperalgesia in which physical coupling of TRPV1 and PI3K in a signal transduction complex facilitates trafficking of TRPV1 to the plasma membrane.

The Journal of General Physiology

INTRODUCTION

Painful thermal and chemical stimuli directly gate the cation channel, TRPV1, which is expressed in neurons with cell bodies in dorsal root ganglia (DRG) and trigeminal ganglia (Caterina et al., 1997). Activation of TRPV1 channels produces an influx of Na^+, which depolarizes the neurons, and Ca^{2+}, which acts as a second messenger with pleiotropic downstream effects. TRPV1 is activated by several agents: temperatures >42°C; extracellular protons, with a pKa of 5.5; anandamide and arachidonic acid metabolites; and capsaicin, the pungent extract from hot chili peppers (for reviews see Caterina and Julius, 2001; Julius and Basbaum, 2001). The importance of TRPV1 in nociception is demonstrated by a study with TRPV1 knockout mice (Caterina et al., 2000). In contrast to wild-type mice, TRPV1 knockout mice drank capsaicin-laced water freely, their responses to painful heat were impaired, and they showed little inflammation-induced hyperalgesia. At the cellular level, cultured DRG neurons from TRPV1 knockout mice were insensitive to capsaicin, heat, and extracellular acidification. Thus, TRPV1 is an essential element in detecting painful thermal and chemical stimuli and a potential target for clinical agents to reduce debilitating pain.

Inflammatory pain is an increasingly prevalent problem in our aging population, and the common therapies (opiates and COX-2 inhibitors) are suboptimal in both safety and efficacy. Understanding inflammatory pain at the level of nociceptors is required in order to develop more effective therapies. The excitability of peripheral nociceptors is modulated by G protein–coupled receptors (GPCRs) and receptor tyrosine kinases (RTKs), which are proposed to sensitize gating of TRPV1 (Cortright and Szallasi, 2004; Suh and Oh, 2005). However, the mechanism by which GPCR and RTK ligands sensitize TRPV1 is unclear.

Nerve growth factor (NGF) is released onto peripheral nerve endings during inflammation (Shu and Mendell, 1999b) and may be retrogradely transported to act at nociceptor cells bodies in the dorsal root ganglia (Campenot and MacInnis, 2004). NGF has been implicated in both diminishing the magnitude of Ca^{2+}-dependent desensitization (Galoyan et al., 2003) and sensitizing TRPV1 in a Ca^{2+}-independent manner (Shu and Mendell, 1999a, 2001; Galoyan et al., 2003). NGF activates a receptor tyrosine kinase, trkA. trkA can, in

Correspondence to Sharona E. Gordon: seg@u.washington.edu

Abbreviations used in this paper: CPZ, capsazepine; DRG, dorsal root ganglia; GPCR, G protein–coupled receptor; HBSS, Hank's buffered saline solution; NGF, nerve growth factor; RR, ruthenium red; RTK, receptor tyrosine kinase; TIRF, total internal reflection fluorescence.

turn, be coupled to three pathways: PLC, PI3K, and MAPK (Wiesmann and de Vos, 2001). In the generally accepted PLC model of hyperalgesia (Chuang et al., 2001; Prescott and Julius, 2003), binding of NGF to trkA is coupled to PLC activation. PLC then hydrolyzes PIP2 to sensitize TRPV1 (Fig. 1, bottom left). Hydrolysis of PIP2 would sensitize TRPV1 because PIP2 is believed to tonically inhibit TRPV1. Inhibition of TRPV1 by PIP2 is proposed to be mediated by direct binding of PIP2 to a site near the C terminus of TRPV1: deletion of this site has been found to eliminate sensitization of TRPV1 by NGF (Prescott and Julius, 2003; Zhang et al., 2005a).

More recent results indicate that TRPV1 sensitization by NGF may not be due solely to PIP2 cleavage by PLC. Two groups found that inhibitors of PI3K, but not of PLC, were effective in blocking NGF-mediated sensitization in dissociated DRG neurons (Bonnington and McNaughton, 2003; Zhuang et al., 2004). PI3K inhibitors similarly blocked NGF sensitization in a mouse hyperalgesia behavioral test (Zhuang et al., 2004). Finally, activation of p38 MAPK has been shown to act downstream of NGF/trkA to increase the protein levels of TRPV1 in nociceptor terminals in a transcription-independent manner (Ji et al., 2002). These results raise the question of whether TRPV1 sensitization by NGF is mediated by both the PLC and PI3K pathways and whether PIP2 plays a role in modulating TRPV1. In this study we have directly tested the PLC model for NGF-mediated sensitization. Here we show that, in contrast to predictions of the PLC model, PIP2 potentiates TRPV1. We further demonstrate that PI3K is physically associated with TRPV1 in a signal transduction complex, PI3K activity is required for NGF-mediated sensitization, and sensitization consists of an increase in the number of channels in the plasma membrane.

MATERIALS AND METHODS

Yeast-2-Hybrid

A pretransformed MATCHMAKER fetal human brain cDNA library in yeast strain Y187 was purchased from CLONTECH Laboratories, Inc. (HY4028AHpACT2). TRPV1 N1-432 was subcloned into the pGBKT7 GAL4DNA-BD vector (CLONTECH Laboratories, Inc.). Y187-compatible mating strain AH109 was transformed with TRPV1 N1-432-GAL4DNA-BD. Library screening was performed by mating. Diploid yeast were plated onto SD/−His/−Leu/−Trp (2% agar, 0.67% yeast N2 base, 20 mg/liter L-ade, 20 mg/liter L-arg, 30 mg/liter L-iso, 30 mg/liter L-lys, 20 mg/liter L-met, 50 mg/liter L-phe, 200 mg/liter L-thr, 30 mg/liter L-tyr, 150 mg/liter L-val) + 3 mM 3-AT to select for diploid colonies expressing the HIS3 reporter. Positive colonies were identified by DNA sequencing, and confirmed by directed 2-hybrid screening of cotransformants.

Cell Culture

HEK293 cells were cultured in DMEM + 10% FBS, 0.3 mM L-glutamine, 0.1 mM nonessential amino acids, and 50 U/ml penicillin with 50 μg/ml streptomycin at 37°C, 5% CO_2. F-11 cells were cultured in F12 medium + 20% FBS, 0.2 mM L-glutamine, 100 μM sodium hypoxanthine, 400 nM aminopterin, 16 μM thymidine (HAT supplement), and penicillin/streptomycin at 37°C, 5% CO_2. Cells were transfected with Lipofectamine 2000 or Lipofectamine (Invitrogen) according to the manufacturer's instructions. Cells were used for electrophysiology on the day after transfection. Cells were used for biochemistry 1–3 d after transfection.

DRG neurons were isolated by manual dissection. C57BL/6 mice were anaesthetized with halothane, decapitated, and their spinal columns were removed. The spinal column was bisected and whole ganglia were excised from the surrounding tissue into Hank's buffered saline solution (HBSS). Ganglia were digested with 20 U/ml papain in papain-activation solution (100 mg/ml L-cys, 0.25 mM EDTA, 375 μM $CaCl_2$, HBSS pH 7.4 with $NaHCO_3$), and then collagenase/dispase (1 mg/ml collagenase, 1 mg/ml dispase II in HBSS). Neurons were dissociated from digested ganglia by manual trituration with a fire-polished, serum-coated glass pipette. Finally, neurons were resuspended in F12 medium + 10% FBS and plated in a small volume onto glass coverslips coated with 20 μg/ml laminin and 20 μg/ml polylysine. After 5 h, the neurons were immersed in fresh medium. Neurons were used for electrophysiology between 5 and 12 h after dissection. Neuronal death due to NGF deprivation was not observed during this time.

Immunoprecipitations

Proteins were extracted for immunoblotting from DRG neurons by cell lysis with DRG lysis buffer (PBS with HALT protease inhibitor cocktail [Pierce Chemical Co.]). An appropriate antibody was added to the lysate and was incubated for minimum of 2 h on a shaker at 4°C. Antibody/protein complexes were then bound to protein G agarose beads using a batch method. The beads were washed three to five times with 1 ml ice cold protein G binding buffer (0.01 M sodium phosphate, pH 7.0, 0.15 M sodium chloride) with 0.1% Triton X-100. Proteins were eluted with laemmli sample buffer + 5% β-mercaptoethanol for gel electrophoresis. We obtained the anti–PI3K-p85β antibody from Abcam, the anti-pan trk antibody from Santa Cruz, the anti-phosphotyrosine antibody from Cell Signaling Technology and the anti-TRPV1 antibody (anti–N-term antibody) used for immunoblotting from Neuromics. For immunoprecipitation we used a custom-made antibody (Covance) raised in rabbits against the sequence CYTGSLKPEDAEVFKDSMVPGEK and affinity purified with the Sulfolink Kit (Pierce Chemical Co.).

HEK293 cell lysates were prepared by solubilization of cultured cells in digitonin buffer (20 mM triethanolamine, pH 8.0, 300 mM NaCl, 2 mM EDTA, 20% glycerol, 1% digitonin + protease inhibitors). Proteins were immunoprecipitated with anti-FLAG M2-agarose beads (Sigma-Aldrich), and eluted with laemmli + 5% β-mercaptoethanol. Proteins were separated by gel electrophoresis and transferred to PVDF membranes. For Western blotting, the membranes were blocked for 1 h in TBS-T pH 7.6 (20 mM Tris, 137 mM NaCl, 3.8 mM HCl, 0.1% Tween 20) with 5% (wt/vol) milk. Primary antibody was diluted according to manufacturer's instruction in TBS-T + milk and the secondary antibody was diluted in TBS-T. Membranes were developed using SuperSignal West Femto Max Sensitivity Substrate (Pierce Chemical Co.) and images obtained using a FluorChem 8000 (Alpha Innotech).

Protein Interaction Assays

PI3K p85α and its domains, except C-SH2, were provided by L. Cantley (Harvard University, Cambridge, MA) as follows: p85α. pGEX-1 Lambda T; N-SH2.pGEX-3X; SH3.pGEX-4T-2; and BCR. pGEX-5X-3. C-SH2 was constructed through PCR using p85α. pGEX-1 Lambda T as a template and oligos (5′-GATGGGATCCCCTACTGGGGAG-3′ and 5′-GAGCTAGGAATTCTTACCGGTAGTGG-3′). pGEX-6X-1 was used to produce GST protein for controls.

N1-432-FLAG.pGEX-6X-1 and all of the above constructs were expressed in the BL21 strain of *Escherichia coli* as previously described (Rosenbaum et al., 2004). After the centrifugation of the overnight cultures at 4,000 rpm for 30 min in 4°C, the pellets were resuspended in LBBA buffer (30 mM HEPES, 500 mM NaCl, 20% glycerol, 1 mM DTT, 0.1 mM PMSF, 2.5 μg/ml DNase) for GSTrap FF purification with an AKTA Prime (GE Healthcare). Full-length PI3K p85α was then further purified by size exclusion chromatography (Superdex 200 HR10-30) with an AKTA Explorer (GE Healthcare). GST was cleaved from TRPV1 N1-432-FLAG using PreScission Protease and eluted from the GSTrap FF column. For the rest of the GST fusion proteins, the induction was performed at 37°C and the cultures were grown until OD600 reached ∼1.5. The pellet from culture was resuspended in PBS with EDTA free-Mini Protease Inhibitor Cocktail Tablets Complete (Roche Applied Science) and 1 mM DTT. The resuspended cells were lysed either by sonication or using an Emulsiflex C-5 (Avestin) and were incubated on a shaker at 4°C for 30 min in the presence of 0.1% Triton X-100. After centrifugation, supernatant was incubated with glutathione-agarose in PBS with 1 mM DTT for 30 min on a shaker at room temperature. After the incubation, the beads were washed extensively with PBS + 1 mM DTT + 0.1% Triton X-100, and the proteins were eluted in GST elution buffer (50 mM Tris pH 8.0, 15 mM glutathione, 0.1% Triton X-100, 1 mM DTT).

TRPV1-FLAG synthesis was performed by transfection and digitonin lysing of HEK293 cells as previously described (Rosenbaum et al., 2004). Both TRPV1-FLAG and TRPV1 N1-432-FLAG were bound to anti-FLAG M2 agarose beads by incubating a minimum of 2 h at 4°C on a shaker. The beads were washed thoroughly to eliminate any unbound FLAG-tagged protein. The beads were then incubated for a minimum of 2 h at 4°C on a shaker in excess with GST fusion proteins. Beads were then washed extensively with PBS + 0.1% Triton, and the bound material was eluted with laemmli + 5% β-mercaptoethanol. Bound proteins and input material were boiled for 5 min and then separated by gel electrophoresis, transferred to PVDF membranes, and detected with anti-GST antibody.

Electrophysiology

Excised inside-out patches were obtained with filamented borosilicate glass pipettes (Sutter BF150-86-10) and heat polished with a micro forge. Pipettes used for patching F-11 cells had a resistance of 1.2–2.5 MΩ. DRG neurons were patched with 2.5–3.5 MΩ pipettes. Symmetrical calcium-free recording solutions (130 mM NaCl, 200 μM EDTA, 3 mM HEPES, pH 7.2) were used in the bath and the pipette. Patches that showed a significant time-dependent loss or increase of capsaicin-induced current were discarded. Patches were voltage clamped and currents recorded with an Axopatch 200B amplifier (Axon Instruments, Inc.) interfaced with a Dell personal computer operating Pulse v. 8.53 (HEKA Elektronik). Capsaicin was applied directly to the patch by an RSC-200 solution exchange manifold (Biologik). Because capsaicin freely equilibrates across the membrane, it could be applied to the intracellular surface of excised patches and to the extracellular surface in perforated patch recordings. Its binding site, however, is believed to be located intracellularly (Jung et al., 1999). Because our perfusion system was designed for large amounts of solution (>5 ml), we used an alternative, though slower, means of applying PIP2. Using a glass pipette to manually flush our 300-μl bath allowed us to use much smaller volumes of this very expensive reagent. The longer bath exchange time of this method accounts for the delay between PIP2 introduction and current potentiation observed in Fig. 2 B. All experiments were performed at room temperature.

Perforated-patch recordings of DRG neurons were performed using filamented borosilicate glass pipettes (3.0–4.0 MΩ) containing intracellular saline solution (110 mM K-aspartate, 30 mM KCl, 10 mM NaCl, 1 mM MgCl2, 50 μM EGTA, 10 mM HEPES, pH 7.2) with amphoterecin B (1 mg/ml; Sigma-Aldrich). Cells were continuously perfused with calcium-free bath solution (145 mM NaCl, 5 mM KCl, 1.5 mM MgCl2, 1 mM EGTA, 10 mM glucose, 10 mM HEPES, pH 7.4) + 0.1% BSA. BSA was not used in total internal reflection fluorescence (TIRF) microscopy experiments due to its interference with image clarity. For wortmannin experiments, the cells were preincubated with wortmannin for 5 min before recording the initial currents measured in Fig. 6. Currents were recorded with either an Axopatch 200B amplifier or an EPC 10 amplifier (HEKA Elektronik) interfaced to a Dell personal computer operating Pulse v. 8.53. All solutions were applied to the cell with an RSC-200 solution exchange manifold.

Phosphoinositide (4,5)-Bisphosphate

DiC16-PIP2 (Echelon Biosciences) was solubilized in tetrahydrofuran:water (4:1), dried under N_2, and resuspended to a stock concentration of 0.5 mM in water by bath sonication for 45 min. Stocks were divided into aliquots and frozen at −80°C. Working solutions were prepared daily by dilution of stock aliquots followed by bath sonication for 40 min. DiC8-PIP2 (Echelon Biosciences) was solubilized in water as a 2.5 mM stock, frozen at −20°C, and used the same day it was diluted from the stock.

Total Internal Reflection Fluorescence Microscopy (TIRF)

F-11 cells were grown on glass coverslips and transfected with TRPV1-eYFP, trkA, and p75. At the time of the experiments, coverslips were transferred to a custom-made open perfusion chamber that allowed us to simultaneously perform perforated-patch voltage clamp. Images (100 ms exposure) were acquired using a through-the-lens Olympus IX-70 microscope equipped with a 60× oil immersion PlanApo lens (numerical aperture = 1.45) and either a Stanford Photonics XR Mega 10 intensified charge-coupled device camera or an Andor iXON camera (Navedo et al., 2005, 2006). We excited eYFP using the 488-nm line of an argon laser. Excitation and emission light were separated using a 500-nm long-pass dichroic mirror. An emission 530-nm band pass filter was placed in front of the camera.

Constant laser intensity, focus, and camera gain were maintained during each experiment. For analysis, we included only cells that did not undergo any measurable migration, displacement, or movement during experiments. The spatially averaged fluorescence intensity (i.e., averaged over the entire region of the cell imaged) was determined using Image J software (http://rsb.info.nih.gov/ij/) and custom software written in IDL language.

Data Analysis

All data were analyzed with Igor Pro. For bar graphs, the height of the bar gives the mean. Errors given in the text and error bars shown in all figures represent the SEM. For electrophysiological measurements, all currents shown are difference currents, in which the current in the absence of capsaicin was subtracted to yield the capsaicin-activated component of the current.

Saturating capsaicin–response current records were prepared for nonstationary noise analysis by fitting the rising phase of the response with a smoothed function of the mean current. The smoothed current was subtracted from the raw current trace, and the variance was calculated from the subtracted trace. The variance was then plotted versus the smoothed function of the mean and fitted with the equation $\sigma^2 = xi - (x^2)/N$, where σ^2 is the variance, x is the mean capsaicin-activated current, i is the unitary channel current, and N is the number of functional channels. The unitary conductance from the fit was verified by fitting the slow rising phase of a subsaturating concentration of capsaicin with the same function. Although this second method could not be used to obtain a reliable estimate of N, it yielded values of i that were nearly identical to those estimated from the saturating current responses.

RESULTS

PIP2 Is a Potentiator of TRPV1, Not an Inhibitor

In the PLC model of NGF-mediated sensitization of TRPV1, PIP2 inhibits TRPV1 and hydrolysis of PIP2 by PLC relieves that inhibition (Fig. 1, bottom left). Important predictions of this model are that decreasing the concentration of PIP2 in the membrane will potentiate TRPV1 and increasing the concentration of PIP2 will inhibit TRPV1. We tested these predictions using the inside-out configuration of the patch-clamp technique to allow direct solution access to the intracellular leaflet of the plasma membrane. We used an F-11 cell expression system to mimic native DRG neurons. F-11 cells were constructed as hybridomas of mouse neuroblastoma (N18TG2) and rat dorsal root ganglion cells and they have been found to preserve many properties of DRG neurons (Francel et al., 1987; Jahnel et al., 2001). In addition, expression of fluorescent TRPV1 appeared reticulate in HEK293 cells but was primarily localized to the plasma membrane in F-11 cells (Jahnel et al., 2001).

To test whether decreasing the PIP2 concentration would potentiate TRPV1, we used polylysine to sequester acidic lipids in the membrane (Rohacs et al., 2002). We held the patches at 0 mV and used pulses to +80 mV to drive current through the open channels. Application of 100 nM capsaicin to the bath activated large, stable currents. Although the PLC model predicts that polylysine will potentiate TRPV1, we found that 30 μg/ml polylysine inhibited the capsaicin-activated currents (Fig. 2 A). The mean reduction of current was 82% (±3%, $n = 7$). The inhibition was not reversed by extensive washing of patches with polylysine-free solutions during the time course of our experiments (the inhibition was reversed by adding exogenous PIP2; see below).

We next applied PIP2 to the intracellular surface of the patches to ask whether it acts as an inhibitor, as suggested by the PLC model, or as a potentiator, as would be expected from the inhibition observed with polylysine. We found that 10 μM DiC16-PIP2 (PIP2) profoundly potentiated the capsaicin-activated current (Fig. 2 B), giving a 46-fold increase in current (±35; $n = 5$). The potentiation reversed partially over tens of minutes, as though PLC or lipid phosphatases were active in the patch. (Note that the different perfusion mechanism used for this experiment produced the delayed onset of potentiation observed in Fig. 2 B; see Materials and methods.) No change in current amplitude was observed in untransfected F-11 cells treated with PIP2 ($n = 5$; Fig. 2 C). A soluble, short-chain PIP2 (DiC8-PIP2) induced potentiation that was rapidly reversed upon removal of DiC8-PIP2 from the bath (Fig. 2 D). Finally, the general TRP channel blocker ruthenium red (RR; 10 μM) blocked the same fraction of the

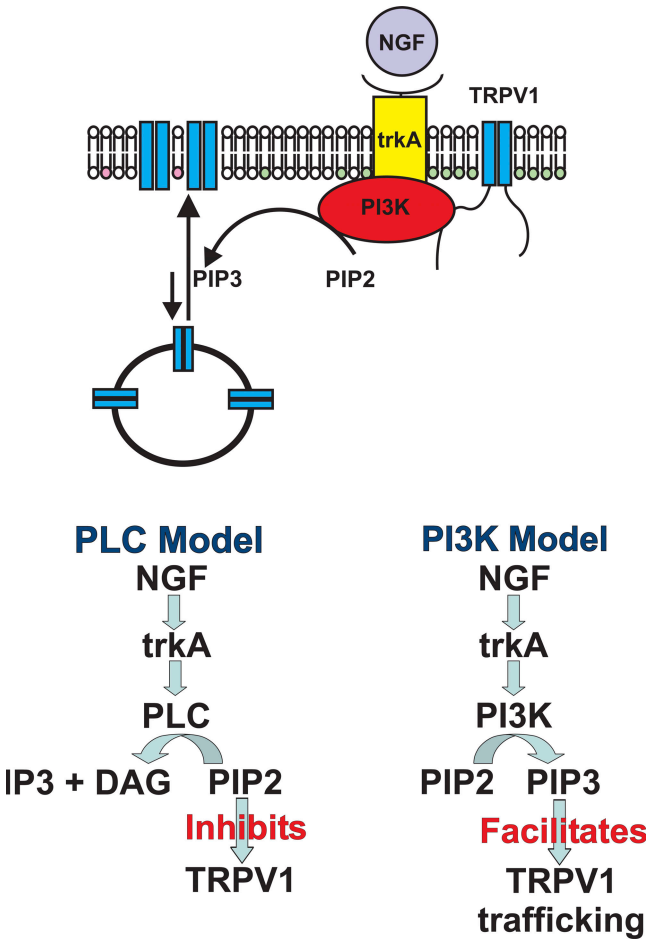

Figure 1. Mechanism of NGF-mediated sensitization. Simplified cartoon representation of the TRPV1-PI3K-trkA signal transduction complex (above) and two models of NGF-mediated sensitization (below). The PIP2 headgroups are shown in green and the PIP3 headgroups are shown in pink.

capsaicin-activated current in the presence and absence of PIP2 ($I_{RR}/I = 0.14 \pm 0.02$, $n = 11$ without PIP2 and $I_{RR}/I = 0.17 \pm 0.02$, $n = 12$ with PIP2) (Fig. 3) and the TRPV1 antagonist capsazepine (CPZ; 10 μM) completely inhibited currents activated by 0.3 μM capsaicin with 10 μM DiC8-PIP2 (Fig. 3), indicating that the PIP2 effects observed were mediated by TRPV1. These data indicate that PIP2 is a potentiator of TRPV1, a result not consistent with the PLC model of hyperalgesia (Fig. 1, bottom left).

Previous experiments testing the effects of reducing the PIP2 concentration on TRPV1 used *Xenopus* oocytes or HEK293 cells (Chuang et al., 2001). Because differences in expression system could potentially affect the polarity of PIP2 modulation, we examined whether PIP2 potentiates or inhibits capsaicin-activated currents in the relevant native tissue. We applied PIP2 to patches from acutely dissociated mouse DRG neurons. In five out of seven patches, PIP2 did not increase the capsaicin-activated current (Fig. 2 E, left;

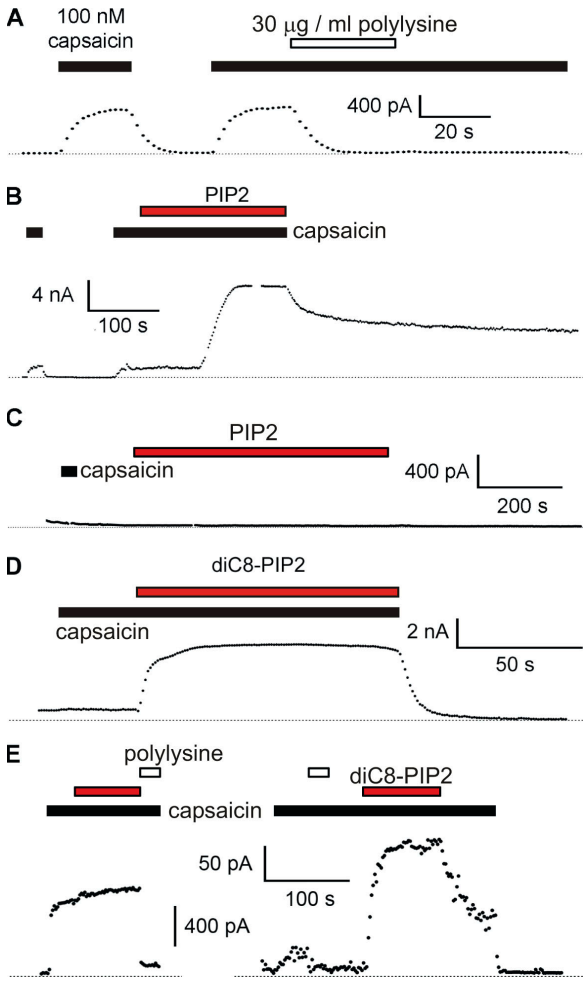

Figure 2. PIP2 is a potentiating molecule for TRPV1, not an inhibitory molecule. (A) Excised inside-out membrane patches were pulled from F-11 cells transfected with TRPV1. Points are steady-state currents recorded during a 100-ms pulse to +80 mV (positive inside relative to outside) from a holding potential of 0 mV. Zero current is indicated by the dotted line. Capsaicin and polylysine (>300 kD) were applied for the duration of the bars. We chose 30 μg/ml polylysine because it has recently been shown to be effective in sequestering PIP2 from TRPM4 channels (Zhang et al., 2005b). Inhibition by polylysine did not spontaneously reverse over the time scale of our experiments, suggesting that its unbinding from the PIP2 is quite slow. (B) Currents and cells as in A. PIP2 (10 μM) and capsaicin were applied during the time of the bar. The delay observed between PIP2 application and the increase in current arose from the special system we devised to apply very small amounts of the expensive phosphoinositide to our cell chamber (see Materials and methods). (C) Application of PIP2 to an untransfected F-11 cell. (D) Water-soluble DiC8-PIP2 (red bar) reversibly potentiated capsaicin-activated current. Inside-out excised patch from F-11 cell transfected with TRPV1. (E) Two representative inside-out patches from mouse DRG neurons. The open and filled black bars as above. The red bar represents DiC8-PIP2. The time scale bar applies to both panels, but each has its own scale bar for current.

the increases in the two other patches were less than twofold). We hypothesized that TRPV1 channels in our DRG neurons were already fully saturated with PIP2 (perhaps because of their low expression levels), so that adding more PIP2 produced little or no additional potentiation. To test this hypothesis, we first applied polylysine to the patches to sequester endogenous PIP2. Our prediction is that if we first eliminate potentiation of TRPV1 by endogenous PIP2, we should be able to restore the potentiation by adding PIP2 to the patches. As in patches from F-11 cells (Fig. 2 A), polylysine treatment decreased the amplitude of the capsaicin-activated current in patches from DRG neurons (Fig. 2 E). We next added DiC8-PIP2 to the patch and found that the potentiation by PIP2 was restored (Fig. 2 E, right; similar results were seen in three patches). Note that the current after PIP2 treatment was larger than observed with capsaicin initially. Our hypothesis predicted that the currents should have been equal. PIP2 has been reported to facilitate recovery of TRPV1 from desensitization (Liu et al., 2005). It is possible that our application of PIP2 caused recovery of desensitized channels in the patch, so that the total number of activatable channels increased. Other potential explanations include nonspecific effects of polylysine and greater activity of DiC8-PIP2 compared with native PIP2. We conclude that PIP2 is not an inhibitor of TRPV1 channels but rather potentiates TRPV1 both in heterologous cells and in native DRG neurons, and is preassociated with TRPV1 in native cells. The potentiation of TRPV1 by PIP2 invalidates the PLC model of NGF-mediated sensitization.

PI3K Interacts Directly with TRPV1

If NGF regulation of TRPV1 does not involve PLC hydrolysis of PIP2, then how does it occur? We hypothesized that, like signaling in the *Drosophila* TRP/TRPL channels (Tsunoda and Zuker, 1999), signaling through TRPV1 could be mediated by a macromolecular signal transduction complex. To identify putative proteins that could bind to TRPV1 in such a complex, we performed a yeast 2-hybrid screen using the N-terminal region of TRPV1 as bait and a human fetal brain library as fish. We found 38 candidate proteins (Table I). For one of these, the p85β subunit of PI3K (PI3K-p85β), we obtained multiple isolates of two independent clones. To confirm the interaction between the N-terminal region of TRPV1 and PI3K-p85β, we performed a directed yeast 2-hybrid assay. Mating of yeast strain AH109 containing GAL4BD-TRPV1-N1-432 (N terminus of TRPV1) with yeast strain Y187 containing GAL4AD-PI3K-p85β enabled the yeast to grow on selective medium requiring expression of the *ade* and *his* reporter genes. Growth of these yeast on selective medium confirmed the interaction between PI3K-p85β and the N-terminal region of TRPV1 in yeast.

Because the yeast 2-hybrid system can yield false-positive results, we tested whether TRPV1 and PI3K-p85β interact in mammalian cells. Our approach was

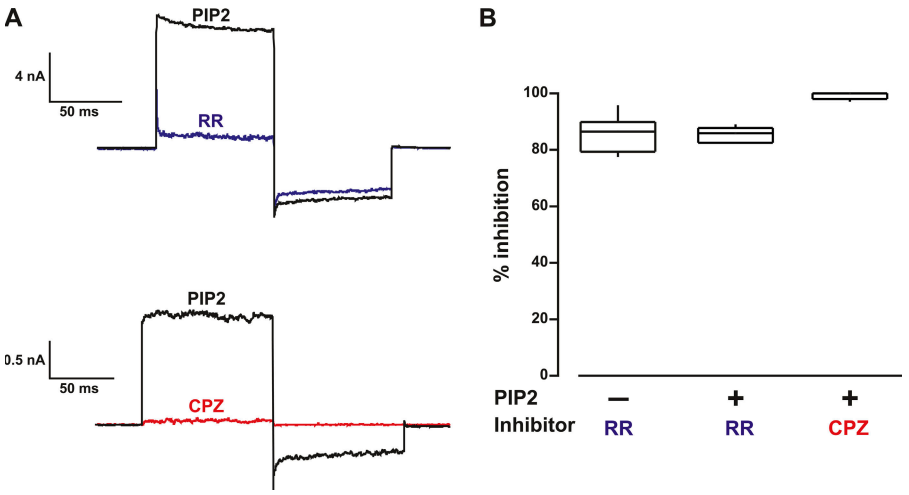

Figure 3. Ruthenium red (RR) and capsazepine (CPZ) reduce the amplitude of PIP2-potentiated currents. (A) Currents from inside-out excised patches in which the membrane was held and 0 mV and the potential was jumped to +80 mV, to −80 mV, and back to 0 mV. Note that RR is believed to be a voltage-dependent blocker of the pore, and thus is less effective at hyperpolarized potentials. In contrast, CPZ may allosterically inhibit activation, giving similar reductions in current at depolarized and hyperpolarized potentials. RR (blue, top) and CPZ (red, bottom) were applied to different patches. (B) Box plot showing the percent reduction in current at +80 mV for RR and CPZ. For comparison, the percent inhibition of capsaicin-activated currents by RR in the absence of PIP2 is shown (first box). Boxes enclose the 25th to 75th percentile of the data, lines within the boxes represent the median, and whiskers extend to the 10th and 90th percentiles.

to use coimmunoprecipitation to test whether PI3K-p85β physically interacts with TRPV1. We transfected HEK293 cells with TRPV1, either wild-type or with a FLAG epitope tag, lysed the cells, and precipitated with an anti-FLAG antibody. We then probed the blot with an antibody against PI3K-p85β. This approach relied on the cell producing endogenous PI3K-p85β in sufficient quantity to interact with overexpressed TRPV1. As shown in Fig. 4 A (left lane), the anti-FLAG antibody precipitated a band of the appropriate size (85 kD) recognized by the anti–PI3K-p85β antibody. This same band was observed when the anti–PI3K-p85 β antibody was used for both immunoprecipitation and immunoblotting (right lane). As a negative control, no PI3K-p85β was observed when non-FLAG tagged channels were used (center lane). We conclude from these experiments that TRPV1 and PI3K-p85β are physically associated in HEK293 cells.

Signaling in heterologous cells is subject to overexpression artifacts and other nonphysiological associations. To determine if TRPV1 and PI3K-p85β interact in native sensory neurons, it was necessary to test whether they could be coimmunoprecipitated from DRG neurons. We homogenized mouse DRGs and used the anti–PI3K-p85β antibody to immunoprecipitate the proteins. We then probed the blot with anti-TRPV1 to visualize TRPV1 that had been immunoprecipitated in the two cases. As shown in Fig. 4 B, the anti–PI3K-p85β antibody brought down TRPV1 (90 kD), indicating that PI3K-p85β and TRPV1 are physically associated in native sensory tissue.

We next sought to determine the region of PI3K-p85 that interacts with TRPV1. The motivation for these experiments arises from the known segregation of function in PI3K-p85. As shown in Fig. 5 A, PI3K-p85 has four types of functional domains: an SH3 domain (blue), a BCR domain for binding small GTP-binding proteins (green), proline-rich domains (purple), and SH2 domains (red). Each type of domain utilizes a different regulatory strategy. Identifying the region of PI3K-p85 that interacts with TRPV1 might therefore provide information essential to understanding how the interaction is regulated.

We performed in vitro interaction assays using TRPV1-FLAG from HEK293 cell lysates immobilized on anti-FLAG beads. We expressed full-length PI3K-p85α, as well as proteins corresponding to each of its functional domains, as GST fusion proteins in bacteria. The α and β isoforms of PI3K-p85 are 57% identical, with even higher identity within each functional domain. For these experiments we used the α subunit because it has been well studied as a GST fusion protein, and we found it to be soluble and largely monodispersed when examined with size exclusion chromatography (unpublished data). Each GST fusion protein was added to the immobilized TRPV1, washed extensively, and the specifically bound protein eluted with denaturing sample buffer. We then ran equivalent amounts of input and the bound protein on an SDS gel and performed Western blot analysis to determine the fraction of each that bound. As shown in Fig. 5 A, TRPV1 from HEK293 cell lysates bound to GST-p85α but not to GST. We next examined which region of PI3K-p85α was involved in the interaction with TRPV1. We found that both SH2 domains (Fig. 5 A, red), but not the BCR domain (Fig. 5 A, green) or the SH3 domain (Fig. 5 A, blue), produced robust binding with full-length TRPV1. The yeast 2-hybrid screen that originally identified PI3K-p85 as a TRPV1 interaction partner identified two independent PI3K-p85 clones, whose locations are represented by the bars in Fig. 5. It is worth noting that these sequences overlap with the SH2 domains, further bolstering the conclusion that the PI3K-p85 SH2 domains mediate the interaction between PI3K and TRPV1.

TABLE I

Proteins Identified in Yeast 2-Hybrid Assay with N Terminus of TRPV1 as Bait

Phosphoinositide-3-kinase regulatory subunit, polypeptide 2 (PI3K-p85β)	Neuronatin
ADO37 protein	NK2 transcription factor homologue B
BN51 temperature sensitivity complementing protein	Nuclear receptor coactivator 6 interacting protein
Catenin, α2	Peroxisome biogenesis factor 10
Catenin, δ2	PL6
Calcium homeostasis ER protein (CHERP)	PLAGL1
Contactin 1	PM5
CRK7	POLR2G
DAZ-associated protein 2	RAB26
Dynactin 1	RAN binding protein 9
GASC1	Ribosomal protein L12
General control of amino acid synthesis 5-like-2 (GCN5)	SMA3
HELO	Small glutamine-rich tetricopeptide repeat (TPR)–containing protein (SGT)
HIV-1 Tat interactive protein	Snapin
HS1 binding protein	Thrombospondin 3
ITM3	Ubiquitin-specific protease 5
LOC90806 similar to RIKEN cDNA 2610307121	VCY-interacting protein 1
Karyopherin, β1	Zinc finger protein 151
Kinesin 2	+11 unidentifiable proteins
Kinesin family member 3B	

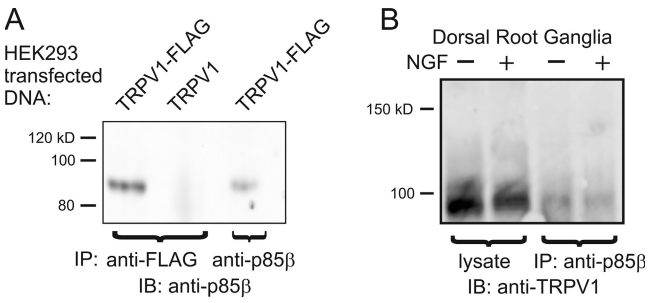

Figure 4. Coimmunoprecipitation between TRPV1 and PI3K-p85β. (A) Immunoprecipitation from HEK293 cells transfected with either TRPV1-FLAG or TRPV1, as a negative control. Proteins were immunoprecipitated with the indicated antibodies, and blots were probed with anti–PI3K-p85β antibody. (B) Immunoprecipitation from mouse DRG cells. Proteins were immunoprecipitated with anti–PI3K-p85β, and blot was probed with anti-TRPV1 antibody.

SH2 domains are common protein–protein interaction domains that bind to phosphorylated tyrosines with high affinity (Vidal et al., 2001). Is tyrosine phosphorylation of TRPV1 required for TRPV1 to interact with PI3K-p85? To address this question we expressed TRPV1, trkA, and p75 (a neurotrophin receptor that complexes with trkA to regulate its function; Schor, 2005) in HEK293 cells (as in Fig. 4 A). We immunoprecipitated with either anti-trkA or anti-TRPV1 antibodies and then used Western blot analysis to probe for trkA and TRPV1 to ensure their expression (Fig. 5 C, top). The membranes were then stripped and reprobed with an anti-phosphotyrosine antibody. As shown in Fig. 5 C (bottom), we found that trkA was tyrosine phosphorylated and that its phosphorylation was increased by NGF treatment (e.g., compare lanes 6 and 7). In contrast, TRPV1 was not recognized by the anti-phosphotyrosine antibody, without or with NGF treatment. We next tested whether recombinant TRPV1 could interact with PI3K-p85α in vitro. We used a FLAG-tagged N terminus of TRPV1 (amino acids 1–432) expressed in bacteria and immobilized on anti-FLAG beads to pull down the recombinant PI3K-p85. We found binding similar to that observed using TRPV1 from HEK293 cells (Fig. 5 A), even though this protein derived from bacteria was not tyrosine phosphorylated (Fig. 5 B). Finally, we asked whether the efficiency of coimmunoprecipitation of TRPV1 and PI3K-p85β was altered by NGF (and, thus, potentially by tyrosine phosphorylation). We found no difference in the intensity of the TRPV1 band observed in anti-p85β antibody precipitates when we treated with NGF (Fig. 4 B). These experiments do not support a role for tyrosine phosphorylation in regulating the interaction between TRPV1 and PI3K-p85 and argue for a persistent interaction between the two proteins rather than a transient one.

PI3K Activity Is Required for NGF-mediated Sensitization

Does the interaction between TRPV1 and PI3K represent a functional macromolecular signal transduction complex? It has been previously shown that wortmannin, a specific inhibitor of PI3K, prevents NGF-mediated sensitization of TRPV1 in calcium imaging experiments (Bonnington and McNaughton, 2003). We tested whether wortmannin would prevent the NGF-mediated increase in TRPV1 currents, thereby indicating that NGF signals through PI3K to regulate TRPV1. We used the perforated patch configuration of whole-cell voltage-clamp recording to measure currents in acutely dissociated mouse DRG neurons. This system allowed us electrical access to the cell's interior and minimized dilution of the cellular contents. Further, using acutely dissociated neurons is expected to yield signal transduction similar to that observed in vivo. As shown in Fig. 6 (A and D), capsaicin-activated currents were stable when examined at 10-min intervals. In contrast, a 10-min incubation with NGF produced highly variable but significant increases in current (Fig. 6, B and D) that is the cellular correlate of sensitization in hyperalgesia. Incubating with NGF and 20 nM wortmannin for 10 min did not produce an increase in the capsaicin-activated current (Fig. 6, C and D). The low concentration

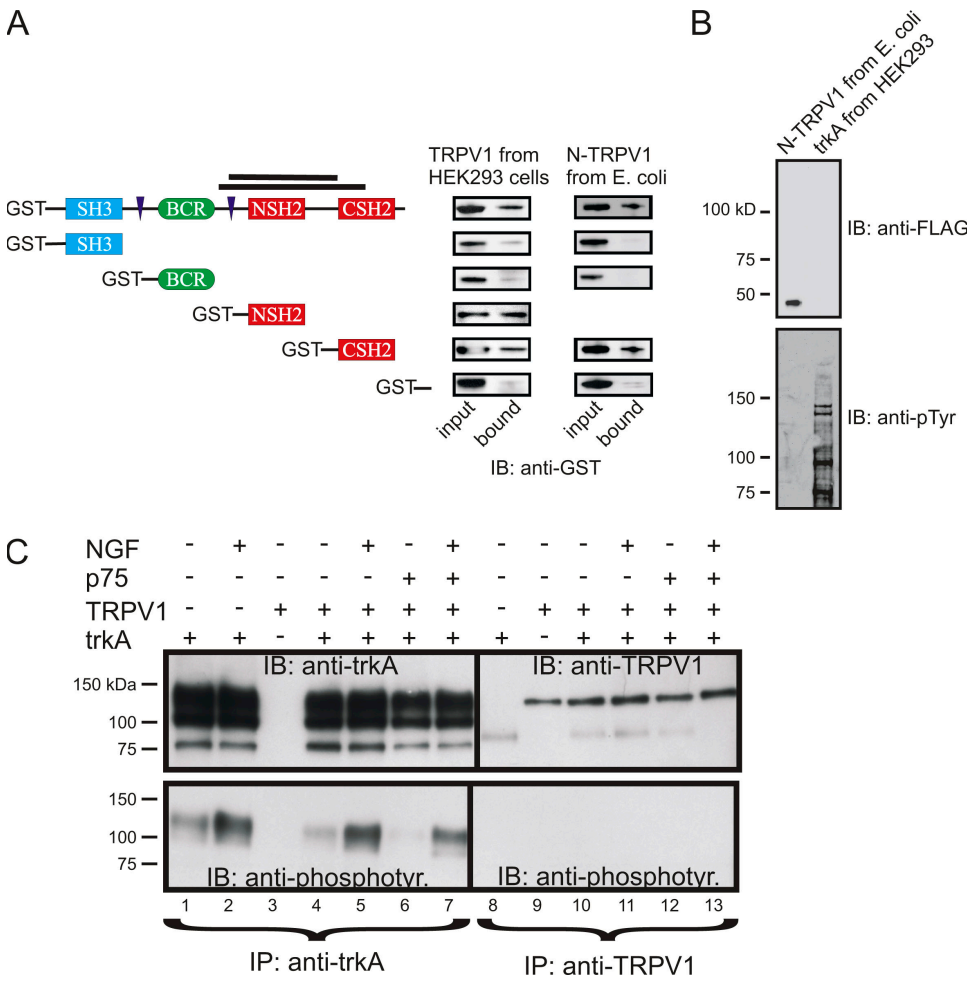

Figure 5. TRPV1 binds to the PI3K SH2 domains in a phosphotyrosine-independent manner. (A) In vitro interaction assay using TRPV1-FLAG from HEK293 cells (left) or recombinant N terminus of TRPV1 from bacteria with a FLAG epitope at its C-terminal end (right). FLAG-tagged TRPV1 protein was immobilized on anti-FLAG agarose beads, and recombinant GST fusion proteins corresponding to PI3K-p85α were tested for interaction. The bars in the cartoon represent the two independent clones of PI3K-p85β identified in the yeast 2-hybrid assay. For the Western blot, equivalent amounts of input and bound proteins were probed with anti-GST antibody. (B) The recombinant N-terminal protein was not tyrosine phosphorylated. The recombinant FLAG-tagged protein was run in the left lane, and lysates from trkA-transfected HEK293 cells were run in the right lane. Duplicate gels were run, and Western blot analysis was then performed with either the anti-FLAG antibody (top) or the anti-phosphotyrosine antibody (bottom). (C) TRPV1 in HEK293 cells was not tyrosine phosphorylated. HEK293 cells expressing combinations of TRPV1, p75, and trkA, as indicated in the figure, were treated with either NGF or vehicle and then immunoprecipitated with anti-trkA (lanes 1–7) or anti-TRPV1 (lanes 8–13) antibodies. Lanes 1–7 were separated from lanes 8–13 and the membranes were probed with anti-trkA antibody and anti-TRPV1 antibody, respectively (top). Segments of the membrane were then reapposed for imaging. The membranes were then stripped and reprobed with anti-phosphotyrosine antibody (bottom).

of wortmannin used here has been shown to be specific for PI3K (Ui et al., 1995). Thus, PI3K activity appears to be required for NGF-mediated sensitization of TRPV1.

NGF Increases the Number of TRPV1 Channels in the Plasma Membrane

An increase in capsaicin-activated current could arise from either potentiation of TRPV1 gating or an increase in the number of active TRPV1 channels in the cell. To distinguish between these possibilities, we examined the effect of NGF on the capsaicin dose–response relation. In perforated-patch experiments, we measured currents activated by various concentrations of capsaicin before and after a 10-min incubation with NGF (Fig. 7 A). We measured the steady-state current at each concentration of capsaicin and constructed dose–response relations (Fig. 7 B). NGF produced a significant increase in the magnitude of the maximal current (Fig. 7 C), with $Imax_{post\text{-}NGF}/Imax_{pre\text{-}NGF} = 1.28$ (±0.07, $n = 10$). In contrast, we found that NGF did not change the EC50 for activation by capsaicin. The mean EC50 value was 49.5 nM (±7.1 nM, $n = 10$) before NGF treatment and 47.8 nM (±12.6 nM, $n = 10$) after NGF treatment, and the mean ratio of EC50 values before and after NGF for individual cells was 0.99 (±0.18, $n = 10$).

The observed increase in macroscopic current could arise from either an increase in unitary conductance or an increase in the number of active channels. We used nonstationary noise analysis to determine which of these parameters was affected by NGF. Fig. 8 A shows the increase in current as capsaicin was applied to an acutely dissociated DRG neuron in a perforated-patch recording before (black) and after (red) treatment with NGF. The time course reflects the perfusion time of our system as the concentration of capsaicin increased from 0 to 300 nM, a saturating concentration for these cells. We applied a smoothing function to determine the instantaneous mean current at each point, and subtracted the smoothed trace to extract the noise (Fig. 8 B). We then plotted the variance of

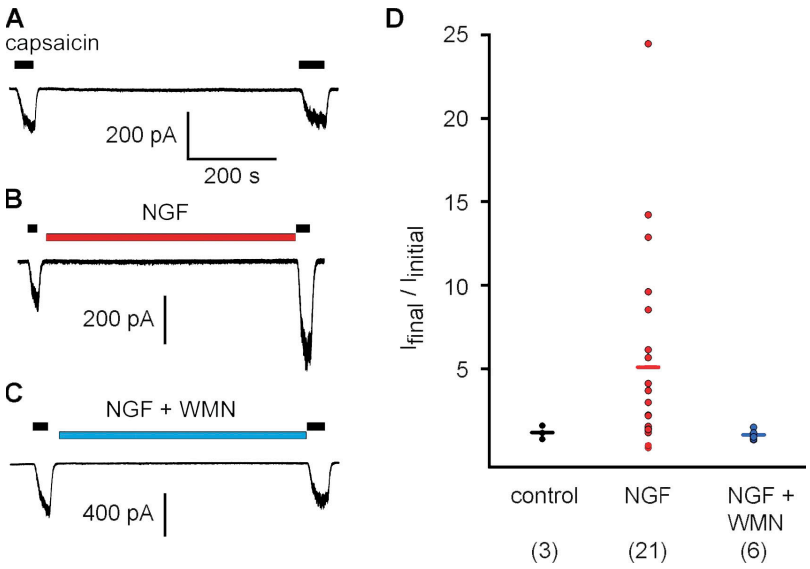

Figure 6. Wortmannin inhibits NGF-mediated sensitization of TRPV1. (A–C) Perforated patch recordings from acutely dissociated mouse DRG neurons activated with 25 nM capsaicin and held at −80 mV. Either (A) no drug, (B) 100 ng/ml NGF, or (C) NGF plus 20 nM wortmannin (WMN) were applied for 10 min. (D) The ratio of final current to initial current for the three conditions. The mean is shown as a horizontal line. The median for these cells was 1.16, 2.99, and 1.05 for control, NGF, and NGF + WMN, respectively.

the noise versus instantaneous mean current (Fig. 8 C) and fitted the data with a parabola with the unitary conductance (i) and number of channels (N) as free parameters (see Materials and methods). The analysis revealed an increase in the number of channels, without a change in either unitary conductance or calculated open probability (Fig. 8 D). The increase in N ($N_{post\text{-}NGF}/N_{pre\text{-}NGF}$ = 1.23 ± 0.07; n = 10) was comparable in magnitude to the increase in current seen in Fig. 7 C. Our data indicate that NGF sensitizes TRPV1 through an increase in the number of active channels in the plasma membrane.

Did NGF activate channels that were already in the membrane but quiescent or increase the total number of channels in the plasma membrane? We used TIRF microscopy to address this question. In TIRF, an exponentially decaying evanescent field allows excitation of fluorescent molecules within ∼100 nm of the coverslip (Axelrod, 2001; Steyer and Almers, 2001). Thus, TIRF microscopy can be used to image plasma membrane–associated fluorescent channels with minimal contamination from the cytoplasm. Using enhanced YFP fused to TRPV1 (TRPV1-eYFP) expressed in F-11 cells, we performed perforated patch electrophysiology experiments simultaneous with TIRF recordings. The two different ways in which NGF could increase channel activity make different predictions about NGF-induced changes in fluorescence. If NGF activates quiescent channels in the membrane, the amplitude of the capsaicin-activated current is expected to increase without an increase in the total number of channels present in the plasma membrane. In this scenario, NGF would lead to an increase in capsaicin-activated current without an accompanying increase in TRPV1-associated fluorescence in the membrane. In contrast, if NGF causes a net increase in the number of channels in the plasma membrane, then an increase in TRPV1-associated fluorescence should be observed that is proportional to the increase in current.

Fig. 9 C shows a set of TIRF images and membrane currents simultaneously recorded from a representative cell under control conditions (left) and upon application of 100 nM capsaicin before (center) and after (right) a 10-min incubation with NGF (100 ng/ml). For these experiments, cells were imaged using identical laser power and camera gain. Changes in fluorescence intensity therefore reflect changes in light emission and not changes in excitation intensity or photon collection efficiency. As expected, superfusion of a solution containing 100 nM capsaicin increased the amplitude of TRPV1 currents. This increase in the amplitude of the currents occurred in the absence of a change in membrane-associated TRPV1-eYFP fluorescence (Fig. 9 C, center, and Fig. 9 D, white bar). Interestingly, incubation with NGF for 10 min increased the magnitude of the capsaicin-sensitive TRPV1 current and TRPV1-eYFP fluorescence ($P < 0.05$). Indeed, NGF increased membrane-associated TRPV1-eYFP fluorescence ($F_{final}/F_{initial}$ post-NGF = 1.3 ± 0.1, n = 5; Fig. 9 D, red bar) and TRPV1 currents (1.3 ± 0.1, n = 4) to a similar extent.

The increase in TRPV1-eYFP fluorescence observed after NGF treatment occurred in the absence of any measurable changes in cell morphology, indicating that the increase in fluorescence was not due to a major reorganization of the amount of membrane within the evanescent field. Furthermore, an increase in TRPV1-eYFP fluorescence was never observed in F-11 cells expressing TRPV1-eYFP, but that were not treated with NGF ($F_{final}/F_{initial}$ post-vehicle = 1.0 ± 0.1, n = 5; see Fig. 8 A). These data exclude the possibility that a time-dependent, NGF-independent mechanism could underlie the increase in TRPV1-eYFP fluorescence described above. In fact, TRPV1-eYFP fluorescence was

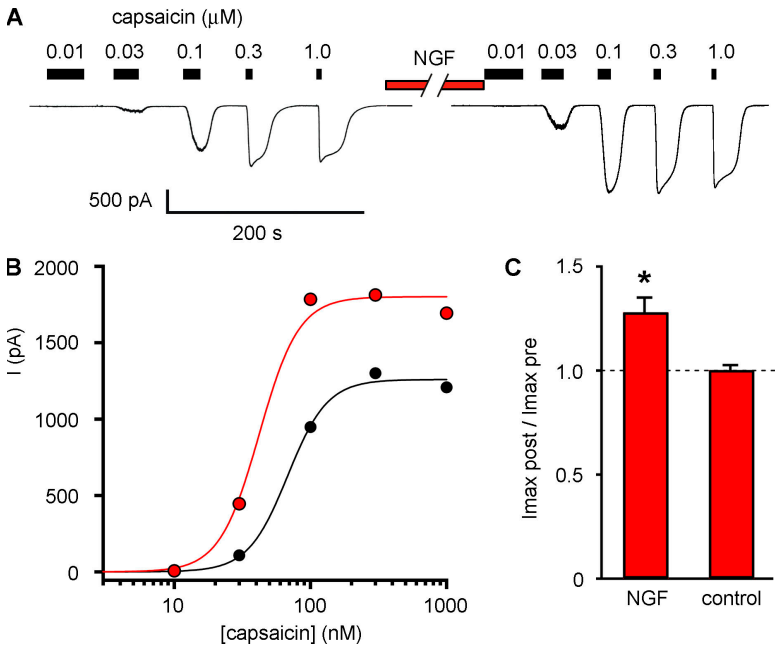

Figure 7. NGF increases the maximum current but not the EC50 for capsaicin. (A) Whole cell currents from acutely dissociated mouse DRG neurons in response to various concentrations of capsaicin before and after a 10-min treatment with 100 ng/ml NGF. (B) Dose–response relation for cell in A. Solid curves are fits with the Hill equation, with a slope of 3. (C) Ratio of maximal currents after 10 min NGF treatment or 10 min control treatment. Asterisk represents a statistically significant difference compared with control. ($Imax_{post\text{-}NGF}/Imax_{preNGF} = 1.28 \pm 0.22$; $n = 10$).

remarkably stable through the progression (10–15 min) of the experiment in the absence of NGF stimulation (Fig. 9 B). We conclude that the NGF-induced increase in TRPV1 current was produced by an increase in the number of functional TRPV1-eYFP channels in the plasma membrane.

DISCUSSION

Thermal hyperalgesia is known to involve an increase in TRPV1 activity (Shu and Mendell, 1999a,b; Chuang et al., 2001), but the mechanism of this increase is controversial. NGF activation of trkA has been proposed to activate PLC, which hydrolyzes PIP2, relieving inhibition of

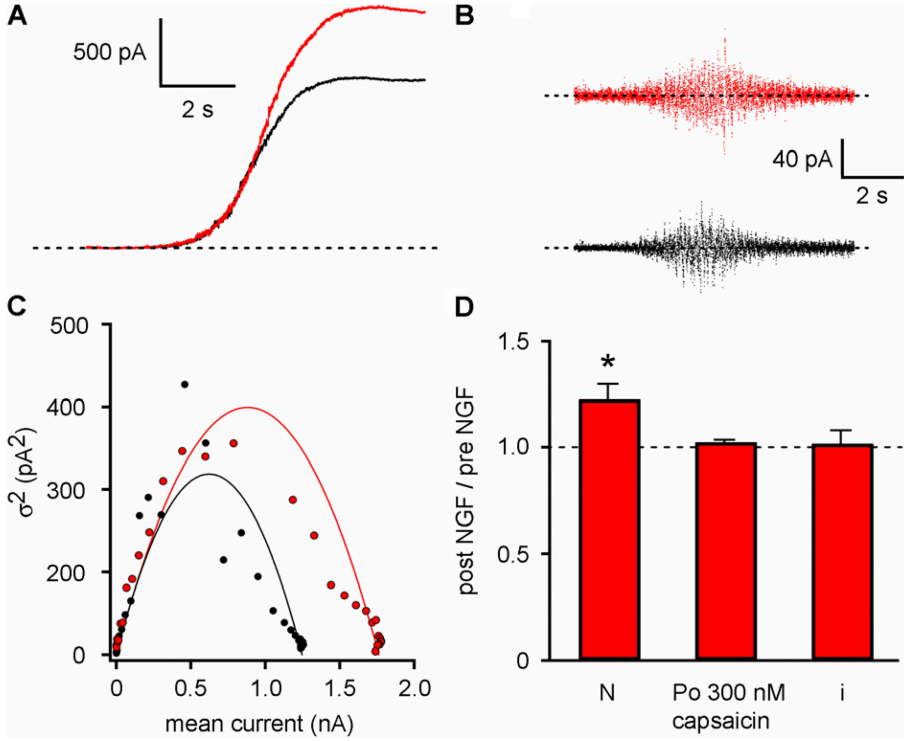

Figure 8. NGF increases the number of functional TRPV1 channels and does not change the channel open probability or unitary conductance. (A) Currents recorded in perforated patch whole cell voltage clamp (−80 mV) were recorded from DRG neurons while they were perfused with saturating capsaicin before (black) and after (red) treatment with NGF (100 ng/ml, 10 min). (B) Smoothed functions of the mean were subtracted from the raw current traces, generating a plot of variance versus time (C). The variance was calculated for segments of data, with the length of the segments reduced until the variance reached a minimum. The variance was plotted versus the smoothed function of the mean and fitted with the equation $f(x) = xi - (x^2)/N$ using a least squares algorithm. (D) The fits revealed an increase in the number of functional channels (N) after NGF, but no difference in i. The absolute value of N was calculated to be 1782 before NGF and 2577 after NGF treatment. The Po was calculated from the capsaicin response current with the equation $P_o = I/(Ni)$. The P_o in saturating capsaicin was not found to have been affected by NGF.

TRPV1 (Fig. 1, bottom left). Three aspects of our work are novel and require reformulation of this model: (1) we found that PIP2 potentiated TRPV1 instead of inhibiting it as predicted by the PLC model; (2) PI3K-p85β was physically and functionally coupled with TRPV1 in a signal transduction complex; and (3) we observed real-time translocation of fluorescent TRPV1 to the membrane upon stimulation by NGF. Based on this evidence, we propose that NGF acts through the PI3K pathway, and not through PLC, to facilitate TRPV1 trafficking to the plasma membrane and hence increase TRPV1 function during hyperalgesia.

A summary of our model is shown in Fig. 1. Here, TRPV1, PI3K, and trkA physically interact in a signal transduction complex (Fig. 1, top). We have included trkA because it has been shown to coimmunoprecipitate with TRPV1 from transfected HEK293 cells (Chuang et al., 2001), a phenomenon we observed as well (unpublished data). Activation of trkA by NGF would facilitate trafficking of TRPV1 to the plasma membrane, increasing channel current (Fig. 9).

Our data are generally consistent with recent work from Zhang et al. (2005a). They show that PI3K inhibitors decrease the number of NGF-sensitive cells, that NGF-treated cells have more TRPV1 present at the surface than untreated cells, and that tyrosine phosphorylation of TRPV1 by Src kinase is in the pathway between trkA and TRPV1. Although tyrosine phosphorylation of TRPV1 was not required for its binding to PI3K-p85 and TRPV1 did not appear to be tyrosine phosphorylated in our system, phosphorylation of TRPV1 makes an attractive component of a system designed to increase TRPV1 trafficking to the plasma membrane. Does phosphorylation of plasma membrane TRPV1 increase its lifetime? Does it help target new channels to regions of the cell that already contain channels? Alternatively, phosphorylation of TRPV1 present in intracellular membrane compartments may be required for their translocation to or insertion in the plasma membrane. It is clear that much work remains to elucidate the mechanism by which NGF signaling increases the number of TRPV1 channels in the plasma membrane.

Here we show that PIP2 promotes TRPV1 activation but also that PI3K, an enzyme that converts PIP2 to PIP3, promotes TRPV1 activation. Although it would be more parsimonious if regulation by PIP2 and by PI3K

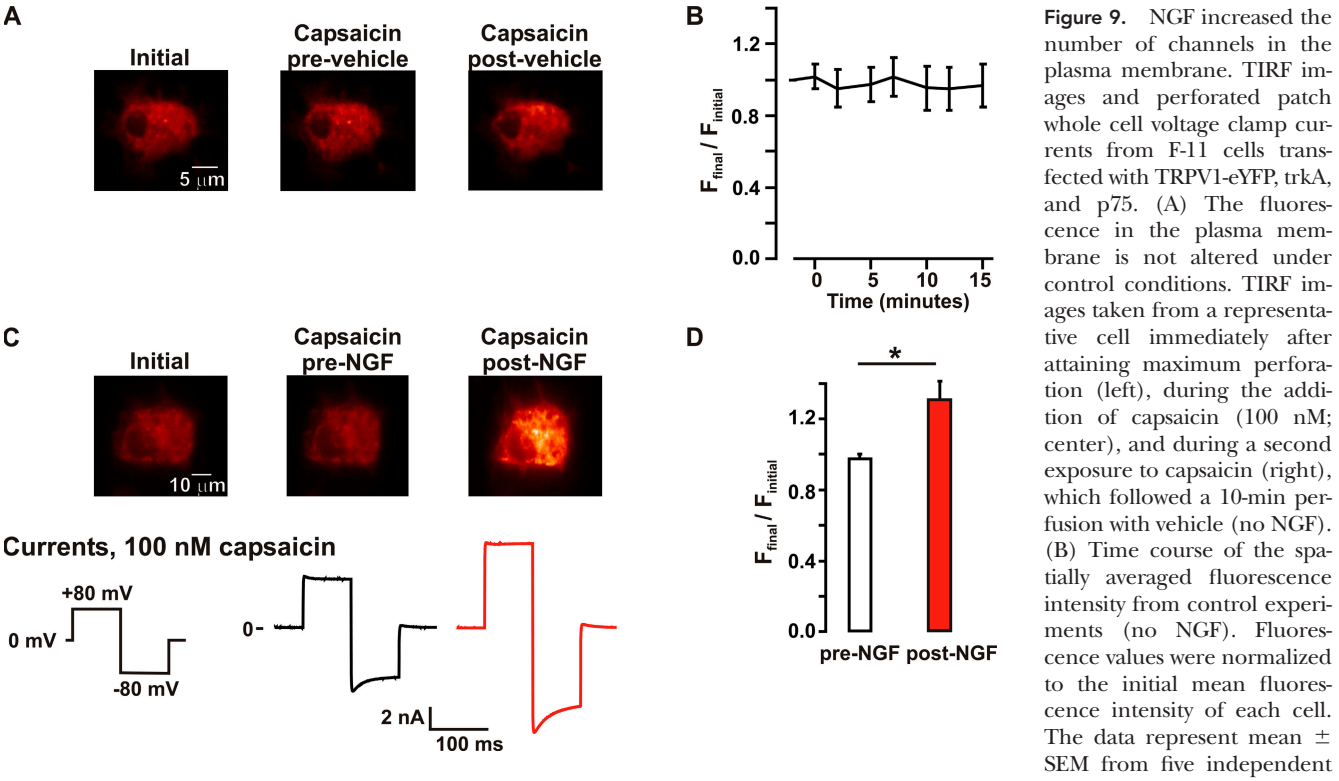

Figure 9. NGF increased the number of channels in the plasma membrane. TIRF images and perforated patch whole cell voltage clamp currents from F-11 cells transfected with TRPV1-eYFP, trkA, and p75. (A) The fluorescence in the plasma membrane is not altered under control conditions. TIRF images taken from a representative cell immediately after attaining maximum perforation (left), during the addition of capsaicin (100 nM; center), and during a second exposure to capsaicin (right), which followed a 10-min perfusion with vehicle (no NGF). (B) Time course of the spatially averaged fluorescence intensity from control experiments (no NGF). Fluorescence values were normalized to the initial mean fluorescence intensity of each cell. The data represent mean ± SEM from five independent experiments. (C) Fluorescence in the plasma membrane increases in response to NGF. TIRF images from a typical F-11 cell after patching (left), during superfusion of capsaicin (center), and during superfusion of capsaicin after stimulation with 100 ng/ml NGF (right) for 10 min. Note that the only difference between the protocol shown on C and A was the addition of NGF. The capsaicin-activated currents correspond to the imaged cell, before (black trace) and after (red trace) NGF treatment. (D) Bar plot of the normalized membrane fluorescence before (white bar) and after (red bar) a 10-min NGF treatment (100 ng/ml). The white bar represents the fluorescence intensity observed during the first capsaicin response (before NGF) normalized to the initial fluorescence. The asterisk represents a statistically significant difference ($P < 0.05$) compared with capsaicin-induced changes pre-NGF treatment ($F_{final}/F_{initial}$ pre-NGF = 0.98 ± 0.03, $F_{final}/F_{initial}$ post-NGF = 1.31 ± 0.11; $n = 5$).

worked via the same mechanism, we do not believe this is the case. Nonstationary noise analysis and TIRF microscopy both indicate that PI3K acts by increasing the number of TRPV1 channels in the plasma membrane. From the increase in fluorescence in TIRF experiments, we believe that the new channels are translocated from beyond TIRF range (100 nm). This translocation mechanism is not likely to be preserved in the excised patch system in which PIP2 potentiation is observed, would not explain how sequestration of PIP2 by polylysine inhibited TRPV1 in excised patches, and would not be expected to be reversed upon washing of DiC8-PIP2 from the bath. We conclude that PIP2 is required for TRPV1 activity, but that the association of PIP2 with TRPV1 is not involved in hyperalgesia. It has been proposed that synthesis of PIP2 is required for recovery from desensitization, with the implication that desensitization of TRPV1 could involve hydrolysis of PIP2 (Liu et al., 2005). The PIP2 potentiation we observed is consistent with such a function. Hyperalgesia, however, would involve a distinct, PI3K-mediated trafficking of TRPV1 to the plasma membrane.

How do we know that the PIP2-activated current is mediated by TRPV1? Four types of experiments, although indirect, together indicate that this is the case. First, PIP2 dramatically potentiated activation of the current by the TRPV1 agonist capsaicin (Fig. 2 B). Second, no effect of PIP2 was observed in untransfected cells (Fig. 2 C). Third, the potentiating properties of PIP2 were observed in both heterologous cells and DRG neurons (Fig. 2, B and E). Finally, the TRPV1 antagonist CPZ completely inhibited currents activated by capsaicin with PIP2, and the nonspecific TRP channel blocker RR blocked the same fraction of the capsaicin-activated current in the absence and presence of PIP2. Thus, although we cannot definitively exclude the possibility that a channel other than TRPV1 was the target of PIP2 potentiation, we see no evidence that PIP2 inhibits TRPV1 as predicted by the PLC model of NGF-mediated sensitization.

PIP2 produced a very large increase in the capsaicin-activated current when TRPV1 was overexpressed in F-11 cells. Given that the open probability of the channels is near 1 at saturating concentrations of capsaicin (Premkumar et al., 2002; Hui et al., 2003; Rosenbaum et al., 2004), this must represent primarily an increase in the number of active channels. These data argue that the vast majority of the channels present in the plasma membrane must be quiescent. In contrast, patches from DRG neurons were not typically potentiated by PIP2 unless first pretreated with polylysine. These data suggest that overexpression of TRPV1 in F-11 cells outstripped the supply of phosphoinositide, so that there was not enough phosphoinositide available for the large number of channels present. The lower expression level in DRG neurons allowed most or all of the channels to be preassociated with PIP2, so that a pool of PIP2-less TRPV1 was not available until the PIP2 had been removed from the channels by polylysine.

PIP2 is a required cofactor for activation of many types of channels. The phosphoinositide modulation of TRPV1 is consistent in many respects with PIP2 modulation of Kir channels, KCNQ channels, TASK and TREK channels, and several TRP channels (Suh and Hille, 2005). In many cases, PIP2 regulation is dynamically controlled by GPCRs and RTKs coupled to PLC. Bradykinin mediates inflammatory hyperalgesia through the B2 GPCR. Although this effect has been proposed to work via a PLC-induced decrease in PIP2, relieving PIP2-mediated channel inhibition, our results are not consistent with such a mechanism. We suggest that TRPV1 sensitization by bradykinin is due to PLC generation of diacylglycerol (DAG), and DAG activation of PKC, a mechanism known to sensitize TRPV1 (Cesare and McNaughton, 1996; Cesare et al., 1999; Premkumar and Ahern, 2000; Vellani et al., 2001; Numazaki et al., 2002; Bhave et al., 2003; Bolcskei et al., 2005; Ferreira et al., 2005; Lee et al., 2005). Further evidence for distinct mechanisms for NGF- and bradykinin-mediated sensitization comes from experiments showing that although bradykinin sensitizes TRPV1 in both adult and neonatal DRG neurons, neurons from early postnatal animals are not sensitized by NGF (Zhu et al., 2004). Finally, mutation of the TRPV1 residues believed to be phosphorylated by PKC upon bradykinin stimulation does not alter NGF-mediated sensitization (Zhang et al., 2005a).

The SH2 domains of PI3K-p85 were sufficient to mediate its interaction with TRPV1, raising the possibility that PI3K-p85 binds to a phosphorylated tyrosine on TRPV1. Work from McNaughton and colleagues (Zhang et al., 2005a) is consistent with this idea. They found that NGF activation of PI3K leads to activation of Src kinase and that this activation was associated with sensitization. Furthermore, phosphorylation of a tyrosine in the N-terminal region of TRPV1 (Y200) by Src was linked with increased surface expression of TRPV1. Although we did not observe tyrosine phosphorylation of TRPV1 under our experimental conditions, and do not believe it is required for PI3K-p85 binding, we cannot rule out that tyrosine phosphorylation of TRPV1 may be important for NGF-mediated sensitization.

The agreement between the magnitude of increases in fluorescence and current in our TIRF/electrophysiology recordings is remarkable. Although at least 10 times slower than the "rapid vesicular insertion of TRP" reported for TRPC5 channels (Bezzerides et al., 2004), the mechanism of NGF facilitation of TRPV1 trafficking may be similar to the mechanism of EGF facilitation of TRPC5 trafficking. A major difference, however, lies in the physical coupling of PI3K and TRPV1. What is the purpose of this coupling? The raison d'être for this signal transduction complex may be to confer spatial or

temporal specificity. In any case, it seems likely that coupling between ion channels and enzymes that control their trafficking is a theme that may be repeated in other systems.

We would like to thank David Julius (University of California San Francisco, San Francisco, CA) for providing the TRPV1 cDNA, Mark Bothwell (University of Washington, Seattle, WA) for providing the trkA and p75 cDNA, and Lewis Cantley (Harvard University, Cambridge, MA) for providing the cDNA of the PI3K-p85-GST fusion constructs. We would also like to thank Mark Bothwell, Bertil Hille, and Bill Zagotta for helpful discussion and Gerry Oxford for comments on the manuscript. We thank Mika Munari and Leslayann Schecterson for expert technical assistance, Josh Burnell and Cristina Tica for DRG isolations, and Dan Beacham and Leon Islas for help with experiments and analysis.

This work was funded by grants from the University of Washington Royalty Research Fund (to S.E. Gordon) and National Institutes of Health (EY013007 and EY017564 to S.E. Gordon, NS07332 to C. Ufret-Vincenty, and HL077115 to L.F. Santana).

Angus C. Nairn served as editor.

Submitted: 15 May 2006
Accepted: 6 October 2006

REFERENCES

Axelrod, D. 2001. Total internal reflection fluorescence microscopy in cell biology. *Traffic.* 2:764–774.

Bezzerides, V.J., I.S. Ramsey, S. Kotecha, A. Greka, and D.E. Clapham. 2004. Rapid vesicular translocation and insertion of TRP channels. *Nat. Cell. Biol.* 6:709–720.

Bhave, G., H.J. Hu, K.S. Glauner, W. Zhu, H. Wang, D.J. Brasier, G.S. Oxford, and R.W. Gereau IV. 2003. Protein kinase C phosphorylation sensitizes but does not activate the capsaicin receptor transient receptor potential vanilloid 1 (TRPV1). *Proc. of Natl. Acad. Sci. USA.* 100:12480–12485.

Bolcskei, K., Z. Helyes, A. Szabo, K. Sandor, K. Elekes, J. Nemeth, R. Almasi, E. Pinter, G. Petho, and J. Szolcsanyi. 2005. Investigation of the role of TRPV1 receptors in acute and chronic nociceptive processes using gene-deficient mice. *Pain.* 117:368–376.

Bonnington, J.K., and P.A. McNaughton. 2003. Signalling pathways involved in the sensitization of mouse nociceptive neurones by nerve growth factor. *J. Physiol.* 551:433–446.

Campenot, R.B., and B.L. MacInnis. 2004. Retrograde transport of neurotrophins: fact and function. *J. Neurobiol.* 58:217–229.

Caterina, M.J., and D. Julius. 2001. The vanilloid receptor: a molecular gateway to the pain pathway. *Annu. Rev. Neurosci.* 24:487–517.

Caterina, M.J., A. Leffler, A.B. Malmberg, W.J. Martin, J. Trafton, K.R. Petersen-Zeitz, M. Koltzenburg, A.I. Basbaum, and D. Julius. 2000. Impaired nociception and pain sensation in mice lacking the capsaicin receptor. *Science.* 288:306–313.

Caterina, M.J., M.A. Schumacher, M. Tominaga, T.A. Rosen, J.D. Levine, and D. Julius. 1997. The capsaicin receptor: a heat-activated ion channel in the pain pathway. *Nature.* 389:816–824.

Cesare, P., and P. McNaughton. 1996. A novel heat-activated current in nociceptive neurons and its sensitization by bradykinin. *Proc. Natl. Acad. Sci. USA.* 93:15435–15439.

Cesare, P., A. Moriondo, V. Vellani, and P.A. McNaughton. 1999. Ion channels gated by heat. *Proc. Natl. Acad. Sci. USA.* 96: 7658–7663.

Chuang, H.H., E.D. Prescott, H. Kong, S. Shields, S.E. Jordt, A.I. Basbaum, M.V. Chao, and D. Julius. 2001. Bradykinin and nerve growth factor release the capsaicin receptor from PtdIns(4,5)P2-mediated inhibition. *Nature.* 411:957–962.

Cortright, D.N., and A. Szallasi. 2004. Biochemical pharmacology of the vanilloid receptor TRPV1. An update. *Eur. J. Biochem.* 271:1814–1819.

Ferreira, J., K.M. Triches, R. Medeiros, and J.B. Calixto. 2005. Mechanisms involved in the nociception produced by peripheral protein kinase c activation in mice. *Pain.* 117:171–181.

Francel, P.C., K. Harris, M. Smith, M.C. Fishman, G. Dawson, and R.J. Miller. 1987. Neurochemical characteristics of a novel dorsal root ganglion X neuroblastoma hybrid cell line, F-11. *J. Neurochem.* 48:1624–1631.

Galoyan, S.M., J.C. Petruska, and L.M. Mendell. 2003. Mechanisms of sensitization of the response of single dorsal root ganglion cells from adult rat to noxious heat. *Eur. J. Neurosci.* 18:535–541.

Hui, K., B. Liu, and F. Qin. 2003. Capsaicin activation of the pain receptor, VR1: multiple open states from both partial and full binding. *Biophys. J.* 84:2957–2968.

Jahnel, R., M. Dreger, C. Gillen, O. Bender, J. Kurreck, and F. Hucho. 2001. Biochemical characterization of the vanilloid receptor 1 expressed in a dorsal root ganglia derived cell line. *Eur. J. Biochem.* 268:5489–5496.

Ji, R.R., T.A. Samad, S.X. Jin, R. Schmoll, and C.J. Woolf. 2002. p38 MAPK activation by NGF in primary sensory neurons after inflammation increases TRPV1 levels and maintains heat hyperalgesia. *Neuron.* 36:57–68.

Julius, D., and A.I. Basbaum. 2001. Molecular mechanisms of nociception. *Nature.* 413:203–210.

Jung, J., S.W. Hwang, J. Kwak, S.Y. Lee, C.J. Kang, W.B. Kim, D. Kim, and U. Oh. 1999. Capsaicin binds to the intracellular domain of the capsaicin-activated ion channel. *J. Neurosci.* 19:529–538.

Lee, S.Y., J.H. Lee, K.K. Kang, S.Y. Hwang, K.D. Choi, and U. Oh. 2005. Sensitization of vanilloid receptor involves an increase in the phosphorylated form of the channel. *Arch. Pharm. Res.* 28:405–412.

Liu, B., C. Zhang, and F. Qin. 2005. Functional recovery from desensitization of vanilloid receptor TRPV1 requires resynthesis of phosphatidylinositol 4,5-bisphosphate. *J. Neurosci.* 25:4835–4843.

Navedo, M.F., G.C. Amberg, V.S. Votaw, and L.F. Santana. 2005. Constitutively active L-type Ca2+ channels. *Proc. Natl. Acad. Sci. USA.* 102:11112–11117.

Navedo, M.F., G.C. Amberg, M. Nieves, J.D. Molkentin, and L.F. Santana. 2006. Mechanisms underlying heterogeneous Ca^{2+} sparklet activity in arterial smooth muscle. *J. Gen. Physiol.* 127:611–622.

Numazaki, M., T. Tominaga, H. Toyooka, and M. Tominaga. 2002. Direct phosphorylation of capsaicin receptor VR1 by protein kinase Cε and identification of two target serine residues. *J. Biol. Chem.* 277:13375–13378.

Premkumar, L.S., S. Agarwal, and D. Steffen. 2002. Single-channel properties of native and cloned rat vanilloid receptors. *J. Physiol.* 545:107–117.

Premkumar, L.S., and G.P. Ahern. 2000. Induction of vanilloid receptor channel activity by protein kinase C. *Nature.* 408:985–990.

Prescott, E.D., and D. Julius. 2003. A modular PIP2 binding site as a determinant of capsaicin receptor sensitivity. *Science.* 300:1284–1288.

Rohacs, T., C. Lopes, T. Mirshahi, T. Jin, H. Zhang, and D.E. Logothetis. 2002. Assaying phosphatidylinositol bisphosphate regulation of potassium channels. *Methods Enzymol.* 345:71–92.

Rosenbaum, T., A. Gordon-Shaag, M. Munari, and S.E. Gordon. 2004. Ca^{2+}/calmodulin modulates TRPV1 activation by capsaicin. *J. Gen. Physiol.* 123:53–62.

Schor, N.F. 2005. The p75 neurotrophin receptor in human development and disease. *Prog. Neurobiol.* 77:201–214.

Shu, X., and L.M. Mendell. 1999a. Nerve growth factor acutely sensitizes the response of adult rat sensory neurons to capsaicin. *Neurosci. Lett.* 274:159–162.

Shu, X., and L.M. Mendell. 2001. Acute sensitization by NGF of the response of small-diameter sensory neurons to capsaicin. *J. Neurophysiol.* 86:2931–2938.

Shu, X.Q., and L.M. Mendell. 1999b. Neurotrophins and hyperalgesia. *Proc. Natl. Acad. Sci. USA.* 96:7693–7696.

Steyer, J.A., and W. Almers. 2001. A real-time view of life within 100 nm of the plasma membrane. *Nat. Rev. Mol. Cell Biol.* 2:268–275.

Suh, B.C., and B. Hille. 2005. Regulation of ion channels by phosphatidylinositol 4,5-bisphosphate. *Curr. Opin. Neurobiol.* 15:370–378.

Suh, Y.G., and U. Oh. 2005. Activation and activators of TRPV1 and their pharmaceutical implication. *Curr. Pharm. Des.* 11:2687–2698.

Tsunoda, S., and C.S. Zuker. 1999. The organization of INAD-signaling complexes by a multivalent PDZ domain protein in *Drosophila* photoreceptor cells ensures sensitivity and speed of signaling. *Cell Calcium.* 26:165–171.

Ui, M., T. Okada, K. Hazeki, and O. Hazeki. 1995. Wortmannin as a unique probe for an intracellular signalling protein, phosphoinositide 3-kinase. *Trends Biochem. Sci.* 20:303–307.

Vellani, V., S. Mapplebeck, A. Moriondo, J.B. Davis, and P.A. McNaughton. 2001. Protein kinase C activation potentiates gating of the vanilloid receptor VR1 by capsaicin, protons, heat and anandamide. *J. Physiol.* 534:813–825.

Vidal, M., V. Gigoux, and C. Garbay. 2001. SH2 and SH3 domains as targets for anti-proliferative agents. *Crit. Rev. Oncol. Hematol.* 40:175–186.

Wiesmann, C., and A.M. de Vos. 2001. Nerve growth factor: structure and function. *Cell. Mol. Life Sci.* 58:748–759.

Zhang, X., J. Huang, and P.A. McNaughton. 2005a. NGF rapidly increases membrane expression of TRPV1 heat-gated ion channels. *EMBO J.* 24:4211–4223.

Zhang, Z., H. Okawa, Y. Wang, and E.R. Liman. 2005b. Phosphatidylinositol 4,5-bisphosphate rescues TRPM4 channels from desensitization. *J. Biol. Chem.* 280:39185–39192.

Zhu, W., S.M. Galoyan, J.C. Petruska, G.S. Oxford, and L.M. Mendell. 2004. A developmental switch in acute sensitization of small dorsal root ganglion (DRG) neurons to capsaicin or noxious heating by NGF. *J. Neurophysiol.* 92:3148–3152.

Zhuang, Z.Y., H. Xu, D.E. Clapham, and R.R. Ji. 2004. Phosphatidylinositol 3-kinase activates ERK in primary sensory neurons and mediates inflammatory heat hyperalgesia through TRPV1 sensitization. *J. Neurosci.* 24:8300–8309.